

LUNG DISEASE CLASSIFICATION USING DEEP LEARNING MODELS BASED ON CHEST X-RAY IMAGES

By

Runa Akter

221-25-110

This Report Presented in Partial Fulfillment of the Requirements for the Degree
of Bachelor of Science in Computer Science and Engineering

Supervised By

Mr. Shah Md Tanvir Siddiquee

Assistant Professor

Department of CSE

Daffodil International University

Co-Supervised By

Mr. Narayan Ranjan Chakraborty

Associate Professor

Department of CSE

Daffodil International University



DAFFODIL INTERNATIONAL UNIVERSITY

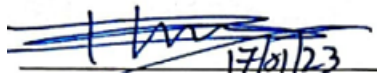
DHAKA, BANGLADESH

17th JANUARY 2023

APPROVAL

This Project/Internship titled “**Lung Disease Classification Using Deep Learning Models based on Chest X-ray Images**” submitted by **Runa Akter, ID No: 221-25-110**, to the Department of Computer Science and Engineering, Daffodil International University has been accepted as satisfactory for the partial fulfillment of the requirements for the degree of M.Sc. in Computer Science and Engineering and approved as to its style and contents. The presentation has been held on 17th January 2023.

BOARD OF EXAMINERS



Chairman

Dr. Touhid Bhuiyan, PhD

Professor and Head

Department of Computer Science and Engineering
Faculty of Science & Information Technology
Daffodil International University

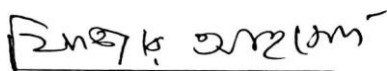


Internal Examiner

Ms. Nazmun Nessa Moon

Associate Professor

Department of Computer Science and Engineering
Faculty of Science & Information Technology
Daffodil International University



Internal Examiner

Dr. Fizar Ahmed

Associate Professor

Department of Computer Science and Engineering
Faculty of Science & Information Technology
Daffodil International University



External Examiner

Md. Safaet Hossain

Associate Professor & Head

Department of Computer Science and Engineering
City University

DECLARATION

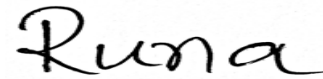
I hereby declare that; this project has been done by me under the supervision of **Mr. Shah Md Tanvir Siddiquee**, and co-supervision of **Mr. Narayan Ranjan Chakraborty**, Assistant Professor, Department of CSE, Faculty of Science and Information Technology, Daffodil International University. I also declare that neither this project nor any part of this project has been submitted elsewhere for award of any degree or diploma.

SUPERVISED BY:



Mr. Shah Md Tanvir Siddiquee
Assistant Professor
Department of CSE
Daffodil International University

SUBMITTED BY:



Runa Akter
ID: 221-25-110

CO-SUPERVISED BY:



Mr. Narayan Ranjan Chakraborty
Associate Professor
Department of CSE
Daffodil International University

ACKNOWLEDGEMENT

First, I express my heartiest thanks and gratefulness to almighty Allah for His divine blessing makes me possible to complete the final year thesis successfully.

I really grateful and wish my profound our indebtedness to **Mr. Shah Md Tanvir Siddiquee, Assistant Professor**, Department of CSE Daffodil International University, Dhaka. Deep Knowledge & keen interest of my supervisor in the field of “Deep Learning” to carry out this thesis. He endless patience, scholarly guidance, continual encouragement, constant and energetic supervision, constructive criticism, valuable advice, reading many inferior drafts and correcting them at all stage have made it possible to complete this project.

I would like to express my heartiest gratitude to almighty Allah and professor dr. Touhid bhuiyan, Professor and Head, Department of CSE, for his kind help to finish my project and also to other faculty member and the stuff of CSE department of Daffodil International University.

Finally, I must acknowledge with due respect the constant support and patients of my parents.

TABLE OF CONTENTS

CONTENTS	PAGE
Approval Page	ii
Boards of examiners	ii
Declaration	iii
Acknowledgements	iv
Abstract	xi
CHAPTER 1: INTRODUCTION	1-5
1.1 Introduction	1
1.2 Statement of the problem	3
1.3 Motivation	3
1.4 Objectives	4
1.5 Report Layout	5
CHAPTER 2: LITERATURE REVIEW	6-12
2.1 Introduction	6
2.2 Literature Review	6
CHAPTER 3: RESEARCH METHODOLOGY	13-23
3.1 Introduction	13
3.2 Data Collection Procedure	13
3.3 Proposed Methodology	13
3.4 Data Preprocessing	14
3.5 Data Augmentation	15
3.6 Split Dataset	15
3.7 Feature Extraction	15
3.8 Fine Tuning	16
3.9 CNN Architecture	16

3.9.1	Convolutional Layer	17
3.9.2	Pooling Layer	17
3.9.3	Fully Connected Layer (FC)	18
3.9.4	Dropout Layer	18
3.10	Activation Function	18
3.10.1	Relu	18
3.10.2	Softmax	18
3.11	Model Implementation	18
3.11.1	EfficientNetB0	19
3.11.2	DenseNet169	20
3.11.3	DenseNet201	21
3.12	Implementation Requirements	22
3.12.1	Software	22
3.12.2	Tools	22
3.12.3	Hardware	23
CHAPTER 4: EXPERIMENTAL RESULT AND DISCUSSION		24-39
4.1	Evaluation Metrics	24
4.1.1	Accuracy	24
4.1.2	Sensitivity	24
4.1.3	Specificity	24
4.1.4	Precision	25
4.1.5	F1-Score	25
4.2	Parameter Optimization	25
4.3	Confusion Matrix	25
4.4	Results and Discussions	26

4.5.1	EfficientNetB0	27
4.5.2	DenseNet169	30
4.5.2	DenseNet201	33
CHAPTER 5: IMPACT ON SOCIETY, ENVIRONMENT AND SUSTAINABILITY		37-38
5.1	Impact of Society	37
5.2	Impact of Environment	38
5.3	Sustainability Plan	38
CHAPTER 6: CONCLUSION AND FUTURE WORK		39-40
6.1	Conclusion	39
6.2	Scope and Limitations of the study	39
6.3	Future work	40
REFERENCES		41-44

LIST OF FIGURES

3.1	Data Collection	13
3.2	Working Procedure Diagram	14
3.3	CNN Architecture	17
3.4	EfficientNetB0 Architecture	20
3.5	DenseNet169 Architecture	21
3.6	DenseNet201 Architecture	22
4.1	Training and validation accuracy graph for EfficientNetB0	27
4.2	Training and validation loss graph for EfficientNetB0	28
4.3	Confusion matrix for EfficientNetB0	29
4.4	Training and validation accuracy graph for DenseNet169	30
4.5	Training and validation loss graph for DenseNet169	31
4.6	Confusion matrix for DenseNet169	32
4.7	Training and validation accuracy graph for DenseNet201	33
4.8	Training and validation loss graph for DenseNet201	34
4.9	Confusion matrix for DenseNet201	35

LIST OF TABLES

2.1	Comparative Analysis	10
4.1	Augmented Images	26
4.2	Different classes TP, TN, FP, FN	29
4.3	Class-wise performance metrics for EfficientNetB0 model	30
4.4	Different classes TP, TN, FP, FN	32
4.5	Class-wise performance metrics for DenseNet169 model	33
4.6	Different classes TP, TN, FP, FN	35
4.7	Class-wise performance metrics for DenseNet201 model	36

ABSTRACT

In the very recent past, Infectious disease-related sickness has long posed a concern on a global scale. Each year, COVID-19, pneumonia, and tuberculosis (TB) cause millions of deaths because they all affect the lungs. Early detection and diagnosis can help provide chances for better care in all circumstances. A low-cost, simple imaging approach called chest X-ray (CXR) imaging can be used to detect and screen lung abnormalities brought on by infectious diseases such as Covid-19, pneumonia, and tuberculosis. This paper provided a thorough analysis of current deep-learning methods for diagnosing Covid-19, pneumonia, and TB. According to the research papers reviewed, the most widely used deep learning algorithm for detecting Covid-19, pneumonia, and TB from chest X-ray (CXR) pictures is Deep Convolutional Neural Network (DCNN). We compared the proposed DNN to well-known DNNs like EfficientNetB0, DenseNet169, and DenseNet201 in order to more accurately assess how well it performed. Our findings are equivalent to the state-of-the-art, and since the proposed CNN is lightweight, it may be employed for widespread screening in areas with limited resources. From three diverse publicly accessible datasets merged into one dataset, the proposed DNN produced the following accuracies for that dataset: 99.15%, 98.89%, and 97.79% for EfficientNetB0, DenseNet169, and DenseNet201 respectively. The proposed network can help radiologists make quick and accurate diagnoses because it is effective at identifying COVID-19 and other lung infectious diseases using chest X-ray imagery. This paper also gives young scientists a good insight on how to create CNN models that are highly efficient when used with medical images to identify diseases early.

CHAPTER 1

INTRODUCTION

1.1 Introduction

In the very recent past, deep learning models have evolved as a potentially useful method in the discipline of healthcare for the diagnostics of diseases, for example the lung ailment that serves as the focus of this particular work. Models based on deep learning have also demonstrated extremely encouraging outcomes in the assessment of other medical conditions [1]. The healthcare industry is able to perform data analysis at breakneck speeds without sacrificing accuracy as a result of this capability [2]. CNN is a specific deep learning technique that can be utilized to the processing of medical pictures in order to facilitate speedy and accurate decision-making. The fundamental idea behind medical image analysis is to aggregate a number of medical images in order to generate a comprehensive CNN evaluation that is capable of differentiating between chaos and informative clinical findings [3]. The COVID-19 epidemic has led to the usage of deep learning in a variety of different contexts. These abilities include the ability to anticipate overall instances and to identify COVID-19 from coughing sounds or visual data, such as X-rays or CT scans. [4].

In December of 2019, the initial COVID-19 verified incidence was found in Wuhan, which is located within Hubei region of China, From there, this virus began to spread to other nations all over the world [1]. The virus which is causing Covid-19 and spreading the sickness named SARS-CoV-2 virus. The great number of infected individuals will only get a moderate or light respiratory infection, and they'll heal without any particular therapy. However, a few people will develop serious illnesses and need prescribed treatment. People who are older or who already have a health problem, such as diabetes, cardiovascular disease, chronic lung disease, or cancer, have a higher risk of developing a serious illness than younger people who do not already have these problems. [5].

As of today, November 2nd, 2022, the World Health Organization had received reports of 2.04 million overall cases and 29,424 deaths in Bangladesh due to the outbreak of the disease [6]. There is now a shortage of accurate diagnostic tools despite the fact that the COVID-19 disease is currently becoming more widespread on a daily basis. This disease has been found to be the cause of mortality for a sizeable number of individuals all over the world. The airway medium is one of the paths that the virus might use to readily and swiftly travel

throughout the body. To limit the percentage of deaths and verified cases caused with the virus, medical professionals all over the world face a significant obstacle in the identification of the virus [7]. Fast identification of individuals who are contaminated with COVID-19, also the provision of specialized care and therapies, is the most effective method for combating the COVID-19 epidemic. Although the reverse transcription-polymerase chain reaction, also known as RT-PCR, is frequently employed in diagnostic testing for COVID-19, it is important to keep in mind that this approach is insensitive to the virus in its first stages, which will result in additional viral spread [8]. CXR images and CT scans are the greatest options to use in identifying patients exhibiting signs of pneumonia because the test kit is pricey and hard to come by [1].

Pneumonia is an illness that affects the airspaces of the lung, and it can be caused by a variety of different microbial pathogens like as bacteria, viruses, or fungi. The infection can cause a wide variety of signs, some of which include chest tightness, fever, the production of mucus, and coughing. The advancement of the illness is indicated by the opacification of the air space, that may recognize by image diagnosis [9] [10]. According to a prediction made by Johns Hopkins University in 2020, more than one hundred thousand children in Bangladesh under the age of five could pass away from pneumonia during the following ten years [11]. Children with impaired immune systems have a greater likelihood of developing pneumonia than children whose immune systems are strong enough to fight off the infection on their own. In 2019, pneumonia was responsible for the deaths of 740180 kids below five years old. This number represents among all deaths 14 percent of children are under the age of five and 22 percent of them aged between one to five years. [12].

The infectious disease tuberculosis, also referred to as TB, mostly affects the lungs and has the potential to be lethal. When a person coughs or sneezes, they expel into the air tiny droplets containing the bacteria that cause tuberculosis. These droplets are then passed from one person to another. Indicators of tuberculosis lung illness include discomfort in the chest, an unpleasant cough that lasts for three weeks or more, and coughing up blood or phlegm. [13]. According to the Health Minister Zahid Maleque, despite the availability of efficient treatments for tuberculosis (TB), more than one hundred individuals lose their lives to the disease every single day in Bangladesh, and over forty thousand people lose their lives to the disease annually [14].

A radiographic investigation, adequate microbiological problems, and clinical awareness are all necessary components in the diagnostic process for lung infection [15]. Additionally, we require a testing method that is capable of identifying a variety of illnesses, such as tuberculosis, normal pneumonia, and differing degrees of COVID-19 severity. When a patient presents themselves at a medical facility, a number of diagnostic procedures, including X-rays, are carried out in addition to a review of the symptoms exhibited by the patient. The state of the lungs and the progression of the disease can be better assessed with the use of X-ray pictures.

1.2 Statement of the Problem

Our nation's medical system is not yet particularly advanced and effective because it is a developing nation. However, older equipment is occasionally exploited in medical services, leading to inaccurate outcomes. Our healthcare system is not as developed as that in developed nations. Additionally, because of the size of our nation's population, the previous health system was unable to provide patients with proper care. To access quality medical treatment, villagers must relocate to towns. For many patients, it is too late to go from town to village. Due to delayed therapy, the condition worsens. We are aware that waiting for a test report is tedious. In actuality, individuals requiring emergency care frequently encounter difficulties. The main cause of this problem is that present methods for identifying different diseases are not automated. Pneumonia, Covid-19, and tuberculosis diagnoses are frequently time-sensitive and need the expertise of an experienced radiologist. Because of patient pressure, most hospitals lack diagnostic equipment, which causes patients to wait longer for test results. Doctors' reports in some complex circumstances are frequently wrong. Due to the high cost of trained radiologists, many hospitals cannot afford to recruit them. In order to efficiently identify Pneumonia, Covid-19, and Tuberculosis from chest X-ray pictures, we require an automated system.

1.3 Motivation

As we saw during the Covid-19 pandemic, pneumonia, Covid-19, and tuberculosis affect a large number of individuals in poor and developing nations. These diseases are characterized by health issues including filth, congestion, and obesity as well as a lack of access to appropriate medical treatment.

Mortality can be decreased by early diagnosis of tuberculosis, covid-19, and pneumonia. Diagnoses for Pneumonia, Covid-19, and tuberculosis are made using chest X-rays. We must thus rely on a radiologist to make the diagnosis. To lessen our dependency on radiologists, we are creating an automated method for detecting Pneumonia, Covid-19, and tuberculosis. To lessen the burden on patients, physicians, and radiologists is our primary goal.

1.4 Objectives

The primary goal of this project is to create a low-cost, automated tool that allows radiologists and other medical professionals to cross-validate their diagnosis and find probable alternate outcomes.

Other goals are:

- Use the chest X-ray report to swiftly diagnose pneumonia, Covid-19, and TB.
- Develop new models to identify various diseases in the future by learning more about deep learning and artificial intelligence (AI).
- Use a range of Deep Learning and Transfer Learning models for the image classification application.
- More quickly, accurately, and effectively identify patients with Pneumonia, Covid-19, and TB.
- Patients will be able to identify TB, Covid-19, and pneumonia based only on the results of a chest X-ray.
- Make a significant contribution to society and the image accelerating biomedical domain.

1.5 Report Layout

Chapter 1 This section are all about research introduction, statement of the problem, motivation and objectives.

Chapter 2 Calls for the expansion of the current system, which describes the whole perspective of the targeted lung diseases and the comparative analysis.

Chapter-3 Demonstrates the Expected Methodology for our structure which consist of dataset, image preprocessing, augmentation, split dataset, feature extraction, fine tuning, CNN Architecture, activation function and model implementation.

Chapter-4 Explore the evaluation matrix, parameter optimization, confusion matrix, outcome of the research and a concise discussion on it.

Chapter-5 This chapter explains how our research affects society and the environment and also explains the sustainability plan.

Chapter-6 Relate the works of the future that we desire to build on, scope and limitation of the study and conclusion.

CHAPTER 2

LITERATURE REVIEW

2.1 Introduction

While conducting this research, we gathered a number of online research papers for educational purposes. X-rays of the chest provide vital medical information that can aid in the prevention and treatment of hospital patients. When dealing with thousands of medical imaging data, the manual testing process proved inadequate. A significant amount of effort has been invested in the fields of medical disease diagnostics. Numerous researchers employed distinct deep learning algorithms to detect multiple sorts of lung disease utilizing various strategies. In this part, we attempted to provide a summary.

2.2 Literature Review

COVID-Mild, COVID-Medium, COVID-Severe, Normal, Pneumonia, and Tuberculosis were among the six categories from which Mehta & Mehendale [16] gathered 1229 images. cGAN was used to increase the number of pictures, and ResNet50, Xception, and DenseNet-169 were trained to correctly classify them. The problems of imbalanced data and overfit are combated with the help of these photos. They found that the accuracy for training and validation was 98.20 percent and 94.21percent, accordingly. Test accuracy was 93.67 percent for the model.

In order to identify COVID-19 from chest X-rays, Khan et al. [3] suggested employing the Deep CNN model known as CoroNet. The model was initially trained with the ImageNet dataset, and then it was trained with COVID-19 and chest pneumonia X-rays of 1300 pictures obtained from two public datasets. The model was created using the Xception architecture, and it was trained with both datasets. After training and testing on the dataset that was provided, CoroNet got an accuracy of 89.6% overall for four classes (COVID vs Pneumonia bacterial versus pneumonia viral versus normal cases) and a precision of 95% for three classes (COVID versus Pneumonia versus normal cases).

Abiyev & Ismail [1], proposed two CNN models trained on separate datasets. All photographs were resized to 180*180 *3 before training and then normalized to facilitate an easier and quicker learning experience. The first training for the model consisted of pneumonia patients and normal CXR pictures. The second model was educated using transfer

learning with COVID-19, pneumonia, and normal patients taken from the 2nd Chest Xray images. On the basis of the test data, the model achieved 98.3% accuracy, 97.9% recall, 98.3% precision, and 98.0% F1 score.

Yoo et al. [17] tried out a decision tree classifier that uses deep learning to find COVID-19 from CXR pictures. A PyTorch-based convolution neural network was used to train the three binary decision trees in the suggested technique. First, CXR images were put into two groups: normal and abnormal. The 2nd tree found abnormal pictures of TB, whereas the 3rd tree did similar for COVID-19. The 1st and 2nd decision trees were 98 and 80% accurate, accordingly. The 3rd tree was 95% accurate. Prior to training and testing, they utilised 162 pictures of COVID-19 contaminated lungs and transformed them to 1,024*1,024.

Subramaniam et al. [18] suggested a preprocessing and classification technique for identifying lung diseases. X-ray images were segmented using HOG, Haar, and LBP. X-ray lung segmentation can help algorithms detect COVID-19. Evaluate several ways using segmented lungs and intersection over union scores. Preprocessed X-rays identify normal, COVID-19, and pneumonia better than raw images. They employed VGGNet, AlexNet, Resnet, and a DNN to classify respiratory diseases. Findings suggest that DNN outperform other classification models.

Venkataramana et al. [2] used Data augmentation and SMOTE to minimize fitting problems and imbalanced categories. They used a multistage classification system on the chest X-ray pictures to assist medical professionals in making more accurate diagnoses and avoiding incorrectly interpreting cases of tuberculosis and pneumonia. After training the model, the classification accuracy for tuberculosis and pneumonia are 97.4% and 88% respectively. The suggested multilevel categorization technique enhances accuracy by 8 to 10% over current methods.

Using parabolic and hyperbolic CNNs and domain-specific transfer learning, Marginean et al. [4] detected COVID-19 alterations in chest X-ray pictures. They collected COVID-19, pneumonia, TB, and normal chest X-rays. They trained parabolic and hyperbolic networks on normal and pneumonia pictures for differentiating between COVID-19, pneumonia, TB, and normal. DenseNets doubled transfer learning. CheXpert's 14 radiological observations are trained using ImageNet weights (e.g., lung opacity, cardiomegaly, fracture, support devices). Weight-initializing COVID-19 and three other classes. Comparing COVID-19 network

adaptations they concluded Quantitative and qualitative studies show more trustworthy networks.

Chen [19] devised an accurate classification approach for detecting COVID-19 viral patterns utilizing chest x-rays of covid-19 and HOG feature extraction. The suggested system uses Cohen's dataset, which has 60000 photos and 400 chest x-ray images of covid-19 that are positive, with evaluation. The databases include 512*512-pixel photos. The proposed approach works well with limited COVID-19 data. The suggested CNN method finds unique input features inside classes.

Alakus & Turkoglu [20] used deep learning and lab data to create clinical predictive models that try to figure out who is most susceptible to get a COVID-19 disease. figuring out how well their models can predict, they used precision, F1-score, recall, AUC, and accuracy scores. Algorithms were evaluated using 18 lab results from 600 patients, also their accuracy was confirmed with 10-fold cross-validation and train-test split methods. Findings of their experiments show that our predictive models can find COVID19 disease in patients with 86.66% accuracy, 91.89% F1-score, 86.75% precision, 99.42% recall, and 62.50% AUC score.

Horry et al. [21] used transfer learning from deep learning models for detecting COVID-19 in X-Ray, Ultrasound, and CT scan images. They optimized the VGG19 model by comparing it to well-known CNN models for image modalities in order to demonstrate that it could be used to the limited and complex COVID-19 datasets. The chosen VGG19 model, that was significantly tweaked using the relevant parameters, detects COVID-19 as opposed to pneumonia or normal for all three lung imaging types with 86% accuracy for X-Ray, 100% for Ultrasound, and 84% for CT scans.

[22] developed a lightweight (9-layered) DNN to identify lung disorders using chest x-ray images caused by Covid-19, Pneumonia, and Tuberculosis. The recommended deep learning network was 99.87% accurate in the Covid-19 vs healthy dataset, 99.55% in the Pneumonia dataset, and 99.76% in the Tuberculosis dataset. Non-healthy CXR screening accuracy was 98.89% for Covid-19 vs Pneumonia, 98.99% vs tuberculosis, and 100% vs Pneumonia. They compared the suggested deep learning network to ResNet50, ResNet152V4, MobileNetV2, and InceptionV3 to evaluate its performance.

[23] developed DenResCov-19 using chest X-ray images to detect COVID-19, pneumonia, TB, and healthy patients. ResNet-50 and DenseNet-121 compose the pipeline. Due to the fact

that DenseNet and ResNet have orthogonal performance among circumstances, an additional layer of CNN blocks was added to link these two models for improved performance. They tested their proposed network on two-, three-, and four-class classification issues (COVID-19 positive, healthy, pneumonia, and TB). Findings suggest that AUC-ROC is 99.60%, 96.51%, 93.70%, and 96.40%, while F1 is 98.21%, 87.29%, 76.09%, and 83.17% for Datasets DXR1, DXR2, DXR3, and DXR4.

[24] used transfer learning to evaluate different CNN algorithm such as VGG16, ResNet-50, and InceptionV3 for lung disease categorization. They constructed a pipeline that separated CXR images before classifying them and compared it to current frameworks. They showed that pre-trained models and basic classifiers can compete with complicated systems. They verified their methodology on some of the public dataset such as Shenzhen and Montgomery lung disease datasets. InceptionV3-based model virtually tied with the top Shenzhen answer despite being computationally cheaper.

Bharati et al. [25] created a hybrid deep learning system which is a combination of VGG, data augmentation, and STN. They used a dataset of chest X-ray collected from Kaggle's NIH. Full and sample datasets were considered. VDSNet improves precision, recall, F0.5 score, and validation accuracy for complete and sampled datasets. VDSNet's full dataset validation accuracy is 73%, whereas vanilla gray, vanilla RGB, hybrid CNN and VGG, and modified capsule network are 67.8%, 69%, 69.5%, and 63.8%.

ResNet50 and DenseNet were employed by Anitha et al. [26] as a pre-trained classifier model to diagnose lung illnesses. The utilized softmax and sigmoid activation functions The results are promising, with accuracy rate for the ResNet50 model at 86.67% and for DenseNet at 98.33%. Each model's performance is differentiated based on training error and validation accuracy. The categorization indicates that DenseNet outperformed ResNet50.

[27] suggested utilizing a modified version of MobileNet V2 to classify and forecast lung diseases from frontal thoracic X-rays. With the help of metadata, we investigated applying transfer learning. They evaluated the effectiveness of our algorithm against other cutting-edge approaches for classifying pathologies using the NIH Chest-Xray-14 database. AUC statistics were used as the primary comparative method to examine how different classifiers differed from one another. With an average AUC of 0.811 and an accuracy of more than 90%, we can see that the achieved result has a wide range overall.

In this study, Magrelli et al [28] trained four deep-learning models from scratch to identify infants with bronchiolitis and pneumonia. They collected 5,907 photographs using a public dataset and worked on the disease in two sections. In one part they applied the algorithm in healthy vs. bronchiolitis classes and in other part healthy vs. bronchiolitis vs. bacterial pneumonia classes. They employed VGG19, Xception, Inception-v3 and Inception-ResNet-v2 algorithms and got the accuracy with 92.25%, 95.25%, 93.5% and 97.75%.

Table 2.1: Comparative Analysis

	Dataset name	Class	Dataset Size	Model	Accuracy
[16]	Public Dataset	6	1229	ResNet50 Xception DenseNet-169	98.2% 96.02% 97.42%
[3]	Public dataset	4-class (COVID vs Pneumonia bacterial vs pneumonia viral vs normal) 3-Class (COVID vs Pneumonia vs normal)	1300	Coronet	89.6% 95%
[1]	Kaggle dataset, Custom Dataset	2 (pneumonia/normal) 3 (COVID-19/pneumonia/normal)	8761	Binary Classification Transfer Learning	85% 98%
[17]	Shenzen, NIH, Eastern Asia Hospital data, Covid-19 Dataset	2 (normal or abnormal) 2 (TB OR NON-TB) 2(Covid or Non-Covid)	1884	three binary decision trees	98% 80% 95%
[18]	public database	3 (normal/pneumonia/COVID-19)	1200	VGGNet AlexNet Proposed DNN	87.5% 75% 91.4%
[2]	TB and pneumonia dataset, types of pneumonia	2 (TB,pneumonia) 3 (Bacterial, Viral, Covid)	14693	Proposed CNN	96.6% 87.1%

	a dataset				
[4]	Cohen dataset, RSNA pneumonia challenge, Shenzhen	4 (COVID-19, pneumonia, tuberculosis and normal)	15645	DenseNets PDE-Based CNN	88.9% 95%
[19]	Cohen's dataset	3 (normal, COVID-19 positive and Pneumonia)	60000	Statistical Approach CNN Proposed CNN+HOG	82% 85% 92.95%
[20]	laboratory findings	1 (Covid-19)	18	ANN, CNN, LSTM, RNN, CNN, LSTM, CNN, RNN	86%,88% 86.66% 84.16% 84.16% 85.66%
[21]	Public Dataset, NIH Dataset	1 (Covid-19)	2114	VGG16, VGG19 Xception InceptionResNet Inception NASNetLarge DenseNet121 ResNet50V2	79%,87% 76% 73% 75% 64% 74% 75%
[22]	Public Dataset, Kaggle Dataset	3 (Covid-19, TB, Pneumonia)	14757	ResNet50, ResNet152V2, MobileNetV2, InceptionNetV3	95.3% 97% 92% 94.5%
[23]	Public Dataset	2 (pneumonia and healthy), 3(COVID-19 positive, healthy, and pneumonia), 4(COVID-19 positive, healthy, TB, and pneumonia)	6775	DenResCov-19 DenseNet-121 ResNet-50 Inception-V3	99.60% 96.51% 93.70% 96.40%
[24]	Shenzhen Hospital dataset	2 (pneumonia and tuberculosis)	918	VGG16, ResNet-50, InceptionV3	70% 75% 82%
[25]		15	5606	VDSNet Vanilla gray Vanilla RGB Hybrid CNN	73% 67.8% 69% 69.5%

				VGG	63.8%
[26]	Public Dataset	2(pneumonia and Covid-19)		ResNet50 DenseNet	86.67% 98.33%
[27]	NIH Chest-Xray-14 database	14	64699	MobileNet V2	95%
[28]	Public	2 (healthy vs. bronchiolitis) 3 (healthy vs. bronchiolitis vs. bacterial pneumonia)	5,907	VGG19, Xception, Inception-v3 and Inception-ResNet-v2	92.25% 95.25% 93.5% 97.75%
Our Proposed models	Public Dataset	4 classes (Pneumonia, Covid-19, tuberculosis and Normal)	6340	EfficientNetB0, DenseNet169, DenseNet201	99.15% 98.84% 97.79%

CHAPTER 3

RESEARCH METHODOLOGY

3.1 Introduction

We used Deep Convolutional Neural Network and Transfer Learning to leverage the Tensorflow framework to solve the problem of detecting lung disease, which is the main objective of our research. We used a public dataset to train our own dataset.

3.2 Data Collection Procedure

In this study we used three publicly available dataset of chest x-ray images from mendeley data [29], IEEE Xplore [4], covid-chestxray-dataset [30] to classify images of covid-19, tuberculosis, pneumonia and healthy classes. We've created a dataset by combining collecting data from various sources and produce a final dataset with 4 classes which are Covid-19, Pneumonia, Tuberculosis and Normal. Here are some sample images of those classes –

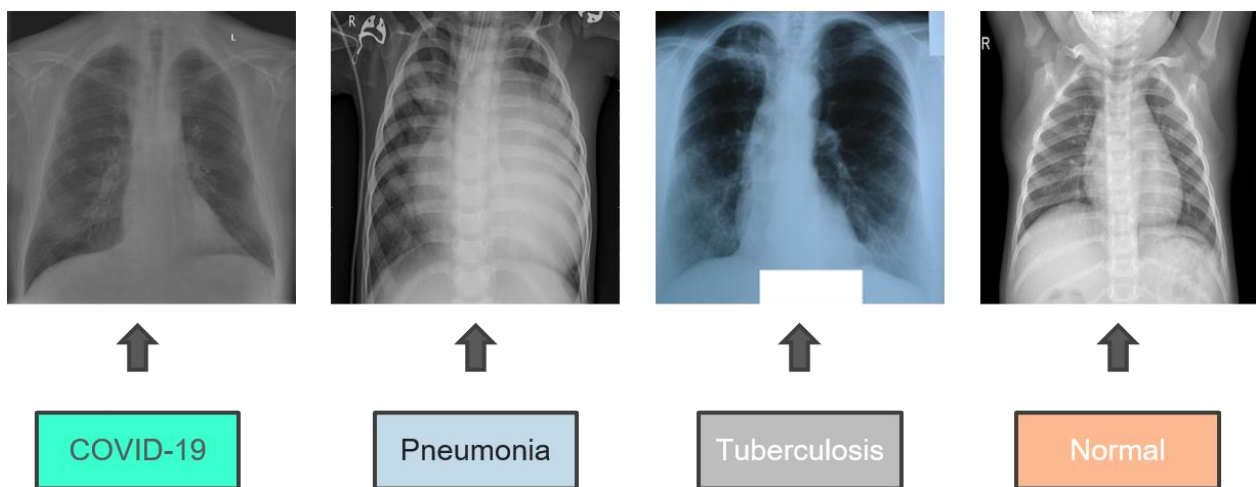


Fig 3.1: Data Collection

3.3 Proposed Methodology

The deep CNN model starts with the gathering of data, then moves on to image preprocessing and augmentation, then separating the dataset into a training and testing portions, feature extraction, in addition lastly the development of the model itself. The step by step working procedure shown below.

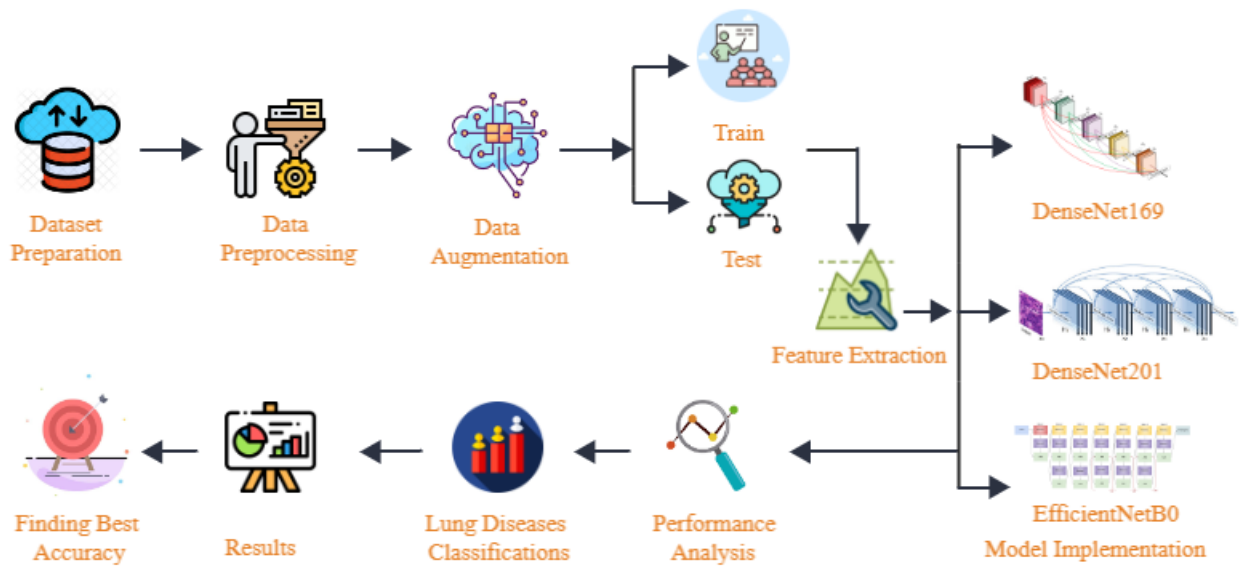


Fig 3.2: Working Pocerure Diagram

3.4 Data Preprocessing

Medical imaging is the practice of generating images of the internal structures of a person's anatomy in order to diagnose various problems. Imaging techniques such as X-rays and CT scans are two of the major prevalent imaging techniques employed detecting lung disorders. The low intensity and contrast of the images, however, make it difficult distinguishing among the images's borders as well as edges, which could result in an incorrect diagnosis in the illness.

To increase the model precision, it is essential to preprocess the clinical data in order to retrieve the relevant info and eliminate any extraneous information [31]. Scaling images, segmenting images, and enhancing images are common pre-processing techniques utilized in the process of illness diagnosis utilizing image modes like X-rays and CT scans [32].

Preprocessing methods employ picture transformations such as rotation, translation, and scaling. Our data collection contains images of varying sizes, posing a difficulty for training purposes. As a result, we have altered the proportions of the image to (224,224). All photos are converted to RGB and jointly analyzed for different models. We rescaled the images and changed the class mode to categorical because none of the images in our dataset were scaled.

3.5 Data Augmentation

The issue of insufficient information can be remedied by the use of an alternative method known as data augmentation. It boosts the amount of samples within the dataset by slightly modifying the current samples [32]. Overfitting can be avoided during the entire preparation procedure with the help of this method. Overfitting occurs when a network overgeneralizes the data it has been given to learn. To attain optimal performance, deep networks demand large volumes of data for training purposes. Most of the time, deep networks need image enhancement to work better when constructing an effective image classifier with limited training data. Artificial training images are generated via image augmentation using a variety of techniques like rotating, shifting, shearing, flipping, and so on. In our dataset we applied specific picture modifications, 3 channel color photos and tagged them in the data pre-processing phase (RGB). We were therefore capable of training the dataset using higher-quality photos and see improved performance. We have also used flipping two times, shuffle, resizing and converted our images mode to categorical in order to achieve the desired results.

3.6 Split Dataset

Data splitting is the procedure of dividing data between a number of categories. Typically, splitting two sections consist of evaluating the information with one part while educating the information in another part. In a straightforward two splitting data parts, the training data set is the one that is used to develop and train classifiers. Test sets are utilized rather frequently in order to assess different parameters and evaluate the effectiveness of a variety of models. The training and test data sets are compared to confirm that the final model functions appropriately. When it comes to machine learning, data is typically separated into three or more sets. The dev set, which is an additional set containing three sets, is used to modify the learning process settings [33]. We have utilized total of 6340 images for the entire experiment while we divided our data into three sections with an 80:15:5 ratio where 5072 images for train the model and 951 images for testing model and 317 images for validation to predict and classify the diseases.

3.7 Feature Extraction

An early collection of raw data is divided up into some more comprehensible categories as part of the dimensionality reduction process known as feature extraction. Therefore, the processing will become more simplified. There are many important variables in this massive

dataset. Processing these variables necessitates a large amount of CPU time. Feature extraction allows for the selection and combining of variables into features, resulting in a significant reduction in data storage. These features are easy to use while correctly and artistically representing the actual data set [34]. Feature extraction compresses image features into a feature vector. Picture registration, object recognition and classification, and content-based image retrieval require accurate image feature representation. The early layers of a deep neural network can intuitively or explicitly express this. [35].

3.8 Fine-Tuning

A procedure that is frequently referred to as "fine tuning" may be used to improve the functionality of a function. A few very little changes that are performed at various points along the process improve the final product. Due to the significance of the adjustment process, even very little modifications can have a big influence on training in terms of the amount of computation time needed, the pace of convergence, and the number of processing units needed. This is due to the significance of the adjustment process. This is true because how things turn out depends so much on the adjusting process. We repeated the fine-tuning procedure several times and tested a wide range of alternative parameter values since we wanted our model to be as accurate as possible. Table 3.8.1 provides an overview of the factors that can be changed during those processes and lists the training and adjustment techniques that produce the best outcomes.

Table 3.1: Fine Tuning

Parameter	Value
Batch Size	30
Steps Per Epoch	50
Epoch	30
Optimizer	Adam, Adamax
Activation Function	Softmax, Relu

3.9 CNN architecture

CNN architecture consists of three principal layers: a convolutional layer, a pooling layer, and a fully connected layer. Fig. X depicts the CNN's underlying layers and architecture. The fully connected layer is responsible for classification, whereas the convolutional and pooling

layers are responsible for extraction of features. In addition to these layers, namely dropout layer and the activation function are two more parameters that are defined. [32].

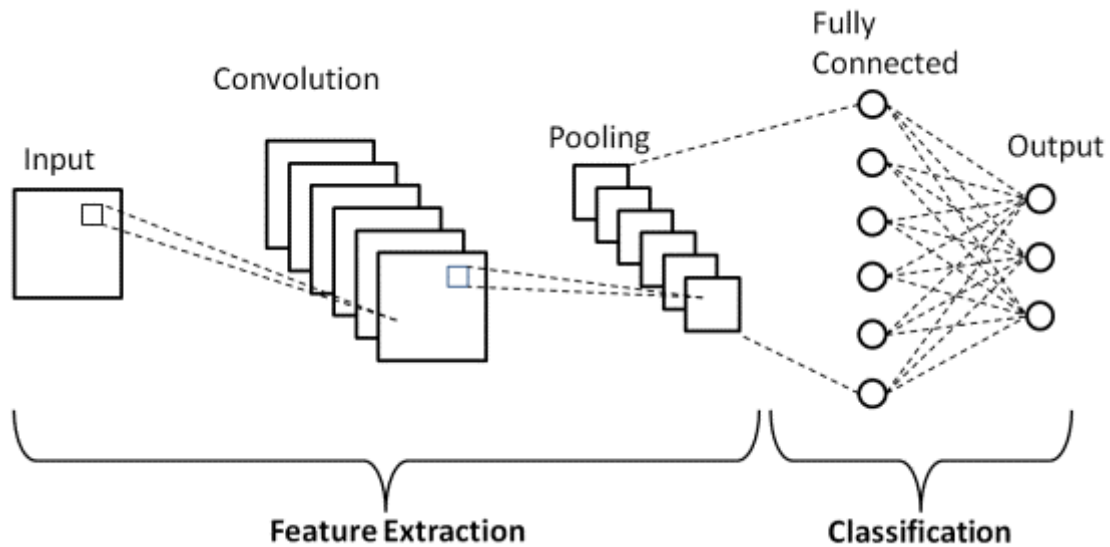


Fig 3.3: CNN Architecture

3.9.1 Convolutional layer

This is the foundational layer, and its responsibility is to eliminate a variety of elements from the input image template. In the convolutional layer, there are some kernels that are only filters. These kernels are scattered across the layer. The kernel, which is simply a smaller matrix than the input data, moves the data from left to right and top to bottom while carrying out a dot function on the data. After everything is said and done, a feature map is produced. The feature maps of the subsequent layers are produced by integrating the feature maps of the preceding layers into the current layer.[41].

3.9.2 Pooling layer

The fundamental objective of pooling is to lessen the extent to which feature maps are utilized, which, in turn, expedites the calculation process by lowering the total number of parameters subjected to training. In addition, pooling can be utilized to merge multiple features into a single comprehensive one. The max pooling operation is the most prevalent sort of pooling operation, and it is the one that is accountable for generating the maximum component from the feature map.

3.9.3 Fully Connected layer

The fully interconnected layer is the final architectural layer (FC layer). Its size is proportional to the output classes it generates. Before picture classification, the fully - connected layer receives information from preceding layers.

3.9.4 Dropout layer

There is a possibility of overfitting occurring when every feature is connected to the fully connected layer. A dropout layer comes in between the input layers and the output layers of a neural network. Its purpose is to reduce the overall size of the model by randomly excluding some neurons from the network. [42].

3.10 Activation Function

To assess whether or not a neuron should be activated, a Neuron Activation Function is used. As a consequence of this, easier statistical methods will be utilized during the procedure of predictions in order to determine whether or not the information that the neuron provides to the network is significant. Typical activation units include the Rectified Linear Unit, also known as ReLu, softmax, sigmoid, and tanh. Among these activation functions, ReLu is by far the utmost popular choice for usage in deep learning models [43].

3.10.1 Relu

ReLU is a non-linear or piecewise linear function that outputs the input directly if it is positive and returns zero otherwise. It is less complicated and more efficient than its predecessors, the sigmoid and tanh.

3.10.2 Softmax

The raw outputs of the neural network are processed by the softmax activation function, which then produces a vector of probabilities from those outputs. This vector of probabilities may be thought of as a probability distribution across all of the input classes.

3.11 Model Implementation

This research had several key objectives, one of the most important of which was to obtain reliable classification findings by utilizing data that was openly accessible to the general public in conjunction with "out-of-the-box" models that included transfer learning. This was done to make up for the small size of the sample data sets as well as to speed up the training

process so that it could be reasonably carried out on hardware that was of a more modest kind.

In order to determine the model that would be best for our research, we concentrated on models that are mostly used, are suitable for transfer learning, and are readily available in packaged form from trustworthy public libraries such as Keras. As a result, we examined only representations of the essential models applicable to this field, as will be detailed in greater detail below. All of these models are conveniently accessible via the Keras Application Programming Interface (API), and they all support transfer learning [36] by enabling the pre-application of ImageNet [37] weights to the model.

3.11.1 EfficientNetB0

Instead of being designed by engineers, the EfficientNet-B0 architecture was created by the neural network itself. They arrived at this model by searching for a multi-objective neural network that simultaneously maximizes accuracy and optimizes floating-point operations. Their search led them to this design. The authors created a full family of EfficientNets, ranging from B1 to B7, with B0 acting as the series' foundational model. In contrast to their competition, these EfficientNets achieved a state-of-the-art level of accuracy on ImageNet while also obtaining very high levels of efficiency. B0 is an easily transportable architecture with eleven million trainable parameters. [38].

As a starting point, we have decided to utilize the EfficientNetB0 baseline model. This model requires an image input with the size 224 224 x 3. Using many convolutional (Conv) layers, a 3x3 receptive field, and the mobile inverted bottleneck Conv layer, the model then extracts information from throughout the layers (MBCConv). Our initial inclination was to select the EfficientNetB0 due to its balanced depths, breadth, and pixel density, which enables it to build a model that is scalable, accurate, and simple to implement. Unlike other kinds of DCNNs, EfficientNetB0 scales each dimension using a specified set of scaling parameters. This technique considerably outperformed earlier state-of-the-art models that were trained on the ImageNet dataset. Even when transfer learning was considered, EfficientNet was still able to achieve great results, demonstrating its applicability beyond the standard ImageNet dataset. Scales ranging from 0 to 7 were included in the initial iteration of the model, signifying a rise in the magnitude of the parameters as well as their precision. Thanks to the most recent release of EfficientNet, users and developers may now access and provide

superior ubiquitous computing equipped with DL capabilities across multiple platforms to meet a wide range of applications [39].

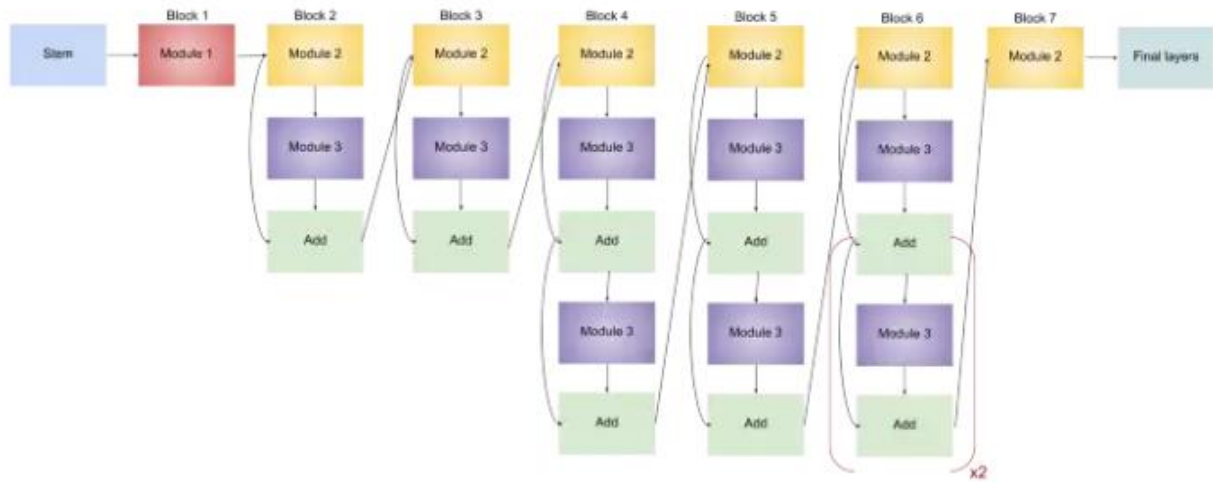


Fig 3.4: EfficientNetB0 Architecture

3.11.2 Densenet-169 model

In 2017, the ImageNet competition was won by the Densenet-169 model, which is a member of the DenseNet family of models and was built by G. Huang et al. [40]. This model was awarded the title of ImageNet champion. In Densenet, the feature maps of all of the layers that come after it receive the additional data that was obtained from all of the layers that came before it. Each layer is accountable for gathering data from the levels that lie above it in the hierarchy. The network might be more condensed and have fewer channels as a result of the fact that each layer is responsible for gathering feature maps from all layers that came before it (and hence improved computational and memory efficiency). Figure X provides a visual representation of the architecture of the Densenet-169. The Densenet-169 model, like like the models that came before it, has been pre-trained using the ImageNet dataset. This ensures that it can accurately recognize images. The DenseNet-169 model was trained using the same dataset, which consisted of 1000 training photos for the Covid19 disease, tuberculosis, pneumonia, and normal conditions, as well as 771 testing photographs and 38 validation images. However, only 805,380 of those parameters can be learned, while the rest 12,642,880 cannot be trained at all. The model includes a total of 13,448,260 parameters. During the

course of the implementation of this approach, the Softmax activation function and the Adamax optimizer were both put into play.

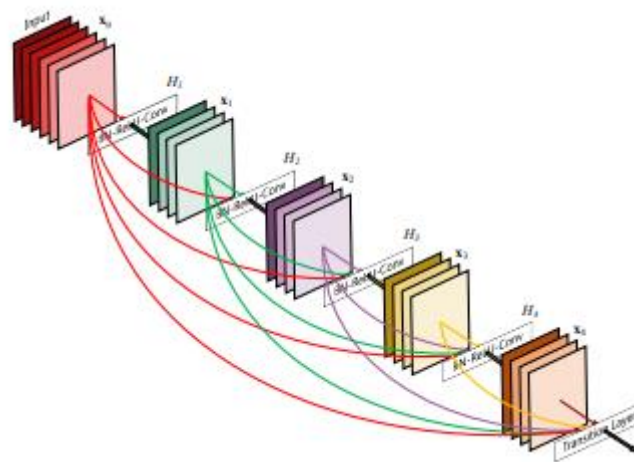


Fig 3.5: DenseNet169 Architecture

3.11.3 DenseNet201 model

The DenseNet201 model was developed during the third phase of the project. This model makes use of transfer learning in order to automatically extract features and weights that were learned from ImageNet. Transfer learning is also used to train the model. The architecture of DenseNet201 makes it feasible to construct models that are both simple to construct and constructed in a manner that is simple to understand. In addition, it is possible to reuse features across levels, which not only improves the effectiveness of the architecture's parameters but also makes it possible for later layers to have a greater diversity of functions and a higher level of speed. Reusing features is one way that this can be performed. Through the utilization of a feed-forward mechanism, one layer of the design is linked to the layer that comes after it. In addition to that, the design of the DenseNet201 model involves the inclusion of a pooling layer as well as a bottleneck structure. This design has the potential to attain better levels of success if the model is made more straightforward and the number of property components is reduced. Within each layer of the DenseNet201 network (BN), nonlinear methods such as convolution (Conv), pooling, rectified linear units (ReLU), and batch normalization have been incorporated (20). An L-layer DenseNet201 network, on the other hand, has $L(L+1)/2$ connections, in contrast to the typical networks. This is due to the fact that the output of each layer acts as the input for the layer that follows it in the hierarchy

(i.e., X0, X1, X2, X3, and X4). One explanation for this phenomenon is that the output of onelayer serves as the input for the layer that comes after it [40].

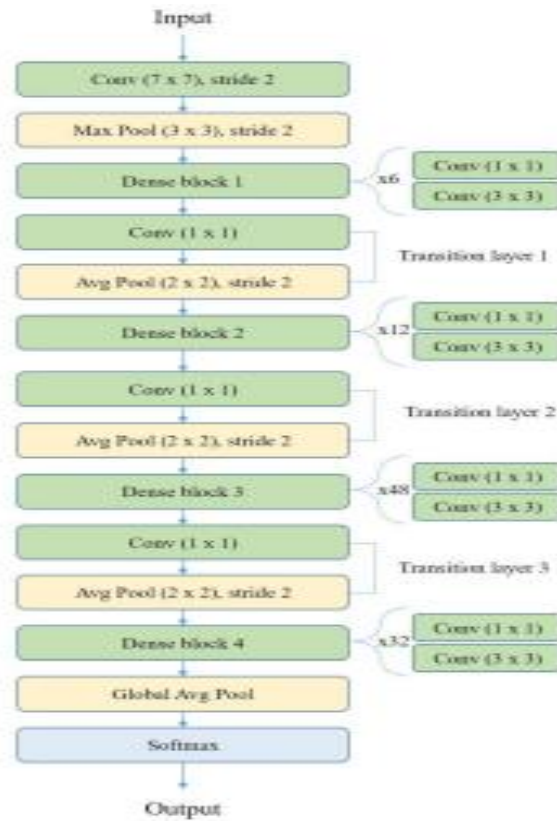


Fig 3.6: DenseNet201 Architecture

3.12 Implementation Requirements

We have chosen a cloud-based platform like Google Colab. It is an enough user-friendly python-based platform and it has huge pre-installed libraries of data science. It took less runtime when the model was building because it gives us free GPU and TPU access.

3.12.1 Software

- Windows 11
- TensorFlow

3.12.2 Tools

- Google Colab
- Jupyter Notebook

3.12.3 Hardware

- Intel core i5 processor
- 8 GB ram
- 1 TB hard disk
- 256 GB SSD
- NVIDIA GeForce GT 1030 GPU

CHAPTER 4

EXPERIMENTAL RESULTS AND DISCUSSION

4.1 Evaluation Metrics

Several distinct criteria of evaluation are applied in the process of determining which of the many models currently available are the most effective in addressing the problem. When it comes to measuring how well a regression model performs, certain evaluation measures do better than others, while others are better suited for use with classification models [1].

4.1.1 Accuracy

This is the most important criterion to take into consideration when contrasting the suggested CNN classifications with the existing ones. The model with the highest accuracy value is the most accurate. In this section, the properties of the confusion matrix are defined and evaluated for assessing the efficacy of the suggested approach. We calculated by the following equation,

$$Accuracy = \frac{Tp + TN}{TP + TN + FP + FN}$$

4.1.2 Sensitivity

The accuracy of the positive prediction is measured by employing these criteria, as well as the outcomes are reported as a fraction of the entire frequency of positives. In addition, the model that has the highest number for its sensitivity is the most sensitive.

$$Sensitivity = \frac{Tp}{TP + FN}$$

4.1.3 Specificity

It is just a replication of the sensitivity test, which is done dividing the total number of negative predictions by the total number of negatives. In addition, the model that has the highest number for its sensitivity is the most sensitive.

$$Sensitivity = \frac{Tp}{TP + FN}$$

4.1.4 Precision

Precision is another evaluation criterion that is typically paired with recall to evaluate the efficacy of classification systems. A forecast result that matches the correctly identified class qualifies as a positive prediction for precision.

$$Precision = \frac{Tp}{TP + FP}$$

4.1.5 F1 Score

The recall and accuracy evaluation metrics are combined into a single evaluation metric called the F1 score performance measure, which is used to assess a classifier's effectiveness. The F1 score evaluation metric is calculated by dividing the result by the sum of the recall and precision evaluation metrics and multiplying the product of precision and recall by two. The F1 score evaluation measure can be computed using the following formula, which explains how it is done.

$$F1\ Score = \frac{2 * precision * recall}{precision + recall}$$

4.2 Parameter Optimization

During the simulation of our suggested model, we focused on a handful of factors to enhance its performance. Here, the batch size has been increased to 30. It boosted the performance of our model. In the instance of the activation function, we employed 'ReLU' and 'Softmax' in order to minimize training loss. We also optimized our model with the help of Adam and Adamax optimizers.

4.3 Confusion Matrix

To maximize the performance of our model, we train it along with multiple image groups and incorporated it into the Deep CNN model's final layer. The most anticipated statistics, including accuracy, sensitivity, specificity, and precision, are displayed using confusion matrices. Confusion matrices are essential because they facilitate the straightforward analysis of values such as true positives, false positives, true negatives, and false negatives. We've utilized confusion matrices in order to assess the performance of our model. Figure X

demonstrates the confusion matrix of the Deep CNN model after training it with the provided images. The diagonal section displays the number of accurately identified photos.

4.4 Results and Discussions

We chose three lung diseases and a healthy class to execute the transfer learning model in order to complete our experimental investigation. Covid-19, pneumonia, tuberculosis, and normal or healthy are our target classes. EfficientNetB0, DenseNet169, and DenseNet201 are three pre-trained transfer learning models that we have deployed.

In the course of our experiment, we first reduced the size of the image to 224 by 224 pixels, and then we performed the augmentation. The Adamax optimizer was utilized, and SoftMax and ReLu activation functions, along with a batch size of 30.

The first thing that we did was begin the process of acquiring images. In order to train the model, numerous phases are developed, such as image pre-processing, which includes runs to resize, filter, augment, and so on and so forth. We used a total of 6340 images for the experiment, dividing our data into three sections with an 80:15:5 ratio so that 5072 images could be used to train the model, 951 images could be used for the testing model, and 317 images could be used for validation. This allowed us to accurately predict and classify the diseases. We examined the confusion matrix for each class as a performance metric for the three applied transfer learning models. This is an effective technique to determine the model that is best suited for the classification task. After that, we also computed other performance measurements such as accuracy, precision, recall, TF, TN, FP, FN and f1 score to find out the best model.

Table 4.1: Augmented images

	Before Augmentation	After Augmentation
Train Data	5072	25360
Test Data	951	4755
Validation Data	317	1585

4.5.1 EfficientNetB0

Figure 7 shows the accuracy over training and validation, while Figure 7 shows the loss over training and validation. The model's ability to learn is illustrated by the train curve, also called the learning curve, which is produced from the training dataset, and its ability to generalize is shown by the validation curve, also called the test curve, which is derived from a hold-out validation dataset.

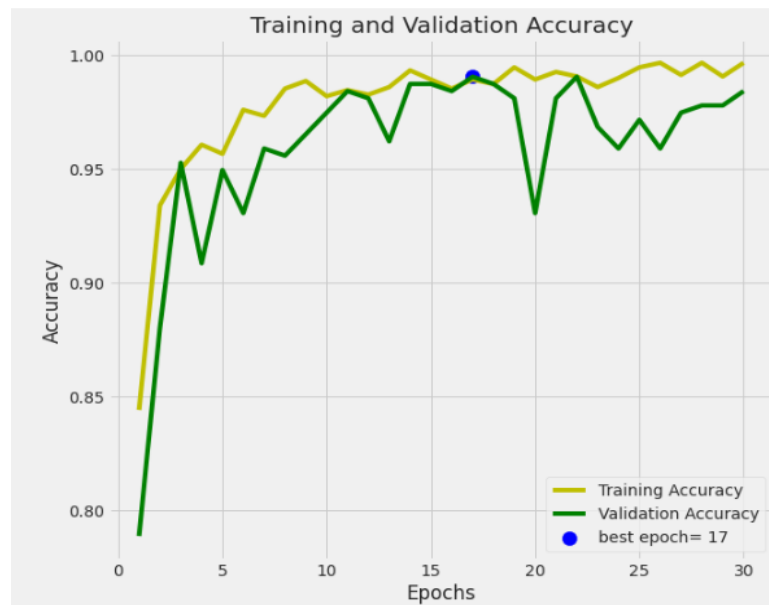


Fig. 4.1: Training and validation accuracy graph for EfficientNetB0 model.

As can be seen from the Fig 7, the accuracy graph is presented with respect to number of epoch in the range between 0 to 1 for 30 epochs for EfficientNetB0 model. We can see both training and validation accuracy increased as time goes. At the early stage the training accuracy and validation accuracy was less. However, the accuracy of training and validation is increasing with the improvement of epoch's number. The graph shows that the model achieved its highest level of accuracy in the 17th epoch. It takes ten seconds to complete the 17th step, which has a learning rate of 0.0010. The findings of the class-by-class evaluation metrics that the EfficientNetB0 model performed are presented in Table 4.5.1.2 for each disease category. It has been observed that the classifier EfficientNetB0 shows the best accuracy for tuberculosis class with 100% precision, recall and F1-Score.

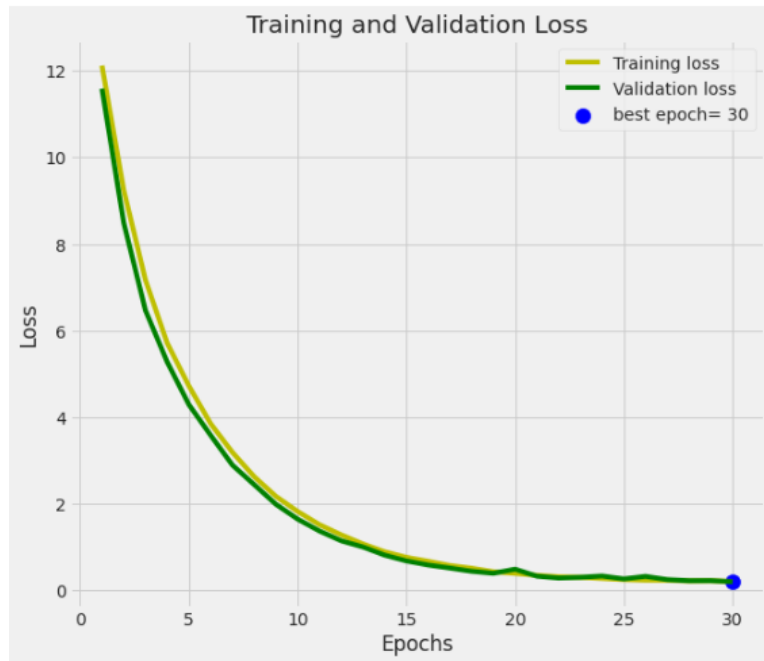


Fig. 4.2. Training and validation loss graph for EfficientNetB0 model.

As observed in Fig. 8, the loss graph for the EfficientNetB0 model is displayed with regard to the number of epochs in the interval between 0 and 1 for 30 epochs. As time passes, we can observe decreasing training and validation loss. The training and validation loss was substantial in the early stages. However, as the number of epochs increases, the loss of training and validation decreases. The graph demonstrates that in the 30th epoch, the model experienced the least amount of loss.

The confusion matrix for EfficientNetB0 model is presented in Figure 9.

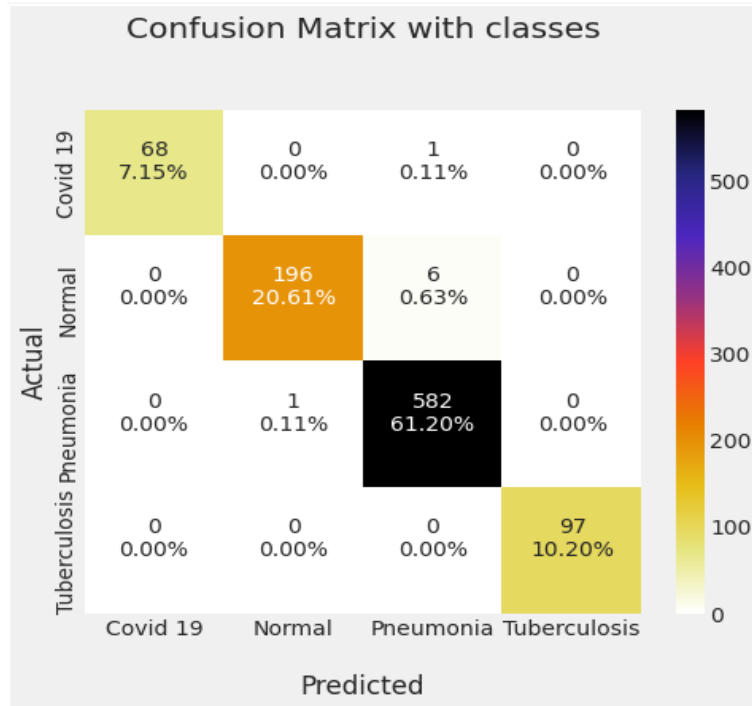


Fig. 4.3: Confusion matrix for EfficientNetB0

The confusion matrix produced by the suggested strategy is shown in Fig. 9 in 5*5 matrix. The result demonstrates that a set of 68, 196, 582 and 97 photos are correctly categorized by the proposed model as Covid-19, Normal, Pneumonia, and Tuberculosis type images. For the purpose of determining the results of the classifier, the values in Table 4.5.1.1 are modified in terms of TP, TN, FP, and FN. For the EfficientNetB0 model, the disease's inaccurate identification rate is noticeably reduced.

Table 4.2: Different classes TP, TN, FP, FN

Different Classes	Covid-19	Normal	Pneumonia	Tuberculosis
TP	68	196	582	97
TN	875	747	361	846
FP	0	1	7	0
FN	1	6	1	0

Table 4.3: Class-wise performance metrics for EfficientNetB0 model.

Model	Class	Precision	Recall	F1 Score	Accuracy
EfficientNetB0	Covid-19	1.00	0.99	0.99	0.99
	Normal	0.99	0.97	0.98	
	Pneumonia	0.99	1.00	0.99	
	Tuberculosis	1.00	1.00	1.00	

According to the table, we are able to deduce that the EfficientNetB0 model is capable of correctly identifying diseases with 99% accuracy, and the maximum precision reserved for the tuberculosis class.

4.5.2 DenseNet169

The graphs demonstrate that the training accuracy and validation accuracy both grew over time. The epoch number is displayed on the x-axis, while the loss in precision or accuracy is shown on the y-axis.

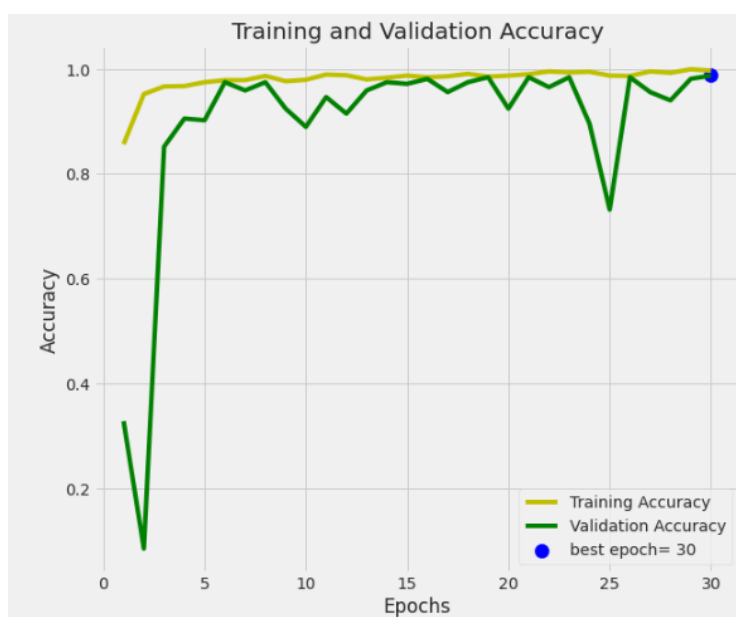


Fig 4.4: Training and validation accuracy graph for DenseNet169 model.

As can be seen from the Fig 10, the accuracy graph is presented with respect to number of epochs in the range between 0 to 1 for 30 epochs for Densenet169 model. We can see both training and validation accuracy increased as time goes. At the early stage the training accuracy and validation accuracy was less. However, the accuracy of training and validation is increasing with the improvement of epoch's number. The graph shows that the model

achieved its highest level of accuracy in the 30th epoch. The findings of the class-by-class evaluation metrics that the DenseNet169 model performed are presented in Table X for each disease category. It has been observed that the classifier DenseNet169 shows the best accuracy for tuberculosis class with 100% precision, recall and F1-Score.

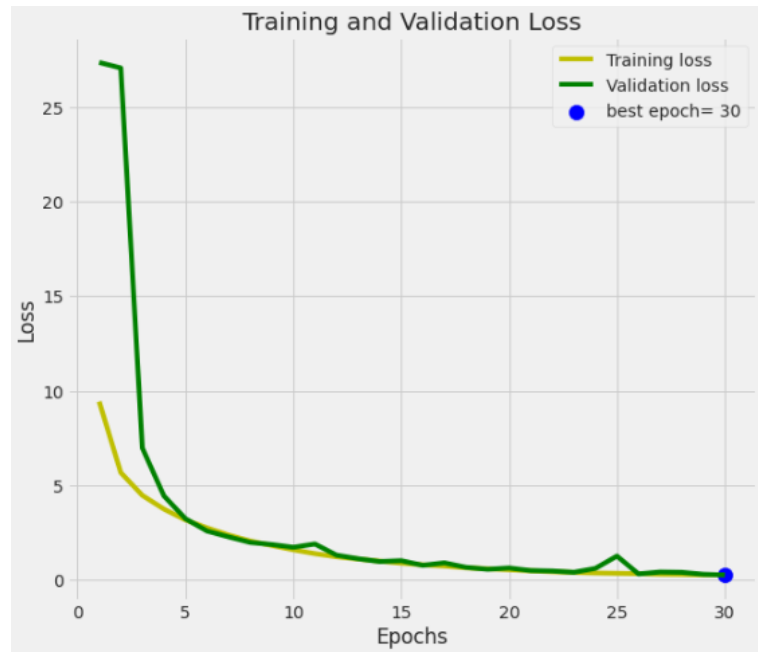


Fig. 4.5. Training and validation loss graph for DenseNet169 model.

As observed in Fig. 11, the loss graph for the Densenet169 model is displayed with regard to the number of epochs in the interval between 0 and 1 for 30 epochs. As time passes, we can observe decreasing training and validation loss. The training and validation loss was substantial in the early stages. However, as the number of epochs increases, the loss of training and validation decreases. The graph demonstrates that in the 30th epoch, the model experienced the least amount of loss.

The confusion matrix for DenseNet169 model is presented in Figure 12.

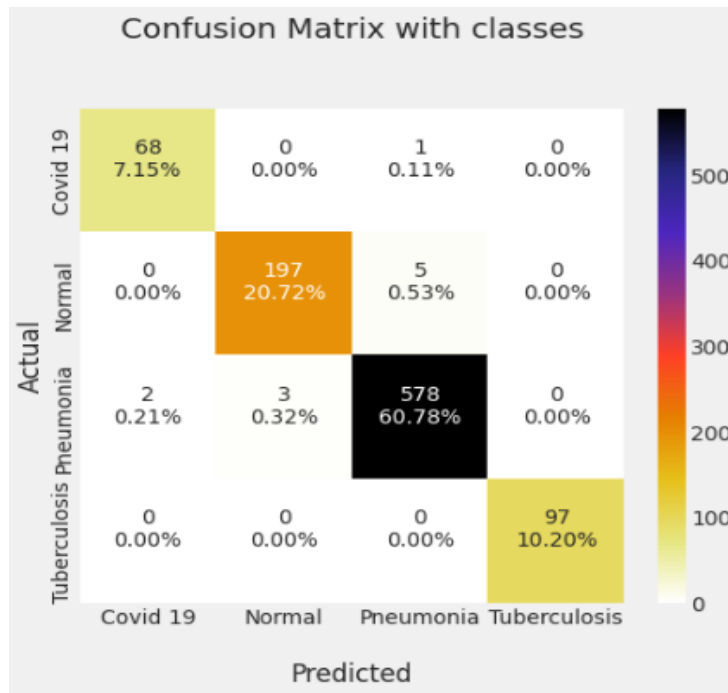


Fig 4.6: Confusion matrix for DenseNet169

The confusion matrix produced by the suggested strategy is shown in Fig. 12. The 5*5 matrix used to illustrate the confusion matrix in Fig. 12 is a very obvious representation. The result demonstrates that a set of 68, 197, 578 and 97 photos are correctly categorized by the proposed model as Covid-19, Normal, Pneumonia, and Tuberculosis type images. For the purpose of determining the results of the classifier, the values in Table 4.5.2.1 are modified in terms of TP, TN, FP, and FN. For the DenseNet169 model, the disease's inaccurate identification rate is noticeably reduced.

Table 4.4: Different classes TP, TN, FP, FN

Different Classes	Covid-19	Normal	Pneumonia	Tuberculosis
TP	68	197	578	97
TN	872	743	362	843
FP	2	3	6	0
FN	1	5	5	0

Table 4.5: Class-wise performance metrics for DenseNet169 model.

Model	Class	Precision	Recall	F1 Score	Accuracy
DenseNet169	Covid-19	0.97	0.98	0.99	0.99
	Normal	0.98	0.98	0.98	
	Pneumonia	0.99	0.99	0.99	
	Tuberculosis	1.00	1.00	1.00	

According to the table, we are able to deduce that the DenseNet169 model is capable of correctly identifying diseases with a rate of 99%, and the maximum precision reserved for the tuberculosis class.

4.5.3 DenseNet201

The graphs demonstrate that the training accuracy and validation accuracy both grew over time. The epoch number is displayed on the x-axis, while the loss in precision or accuracy is shown on the y-axis.

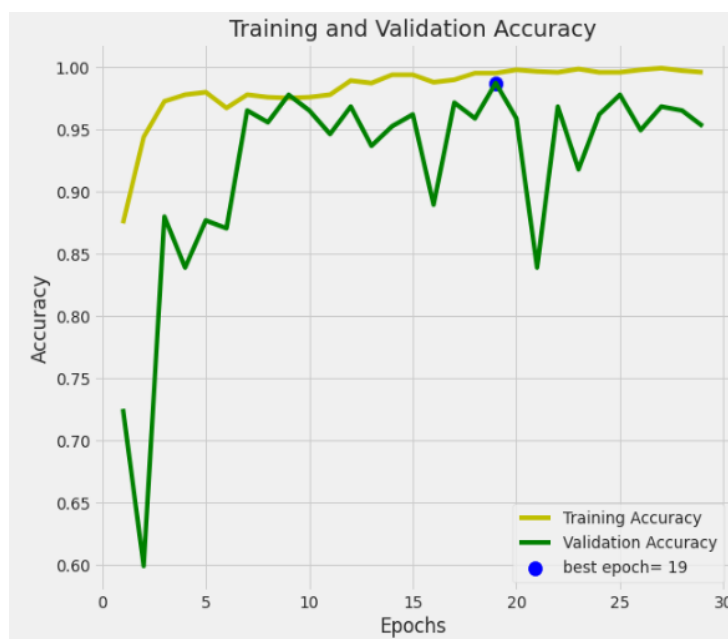


Fig. 4.7: Training and validation accuracy graph for Densenet201 model.

As can be seen from the Fig 13, the accuracy graph is presented with respect to number of epochs in the range between 0 to 1 for 30 epochs for Densenet201 model. We can see both training and validation accuracy increased as time goes. At the early stage the training

accuracy and validation accuracy was less. However, the accuracy of training and validation is increasing with the improvement of epoch's number. The graph shows that the model achieved its highest level of accuracy in the 19th epoch. The findings of the class-by-class evaluation metrics that the DenseNet201 model performed are presented in Table 4.5.3.2 for each disease category. It has been observed that the classifier DenseNet201 shows the best accuracy for pneumonia class with 98% precision, 99% recall and 99% F1-Score.

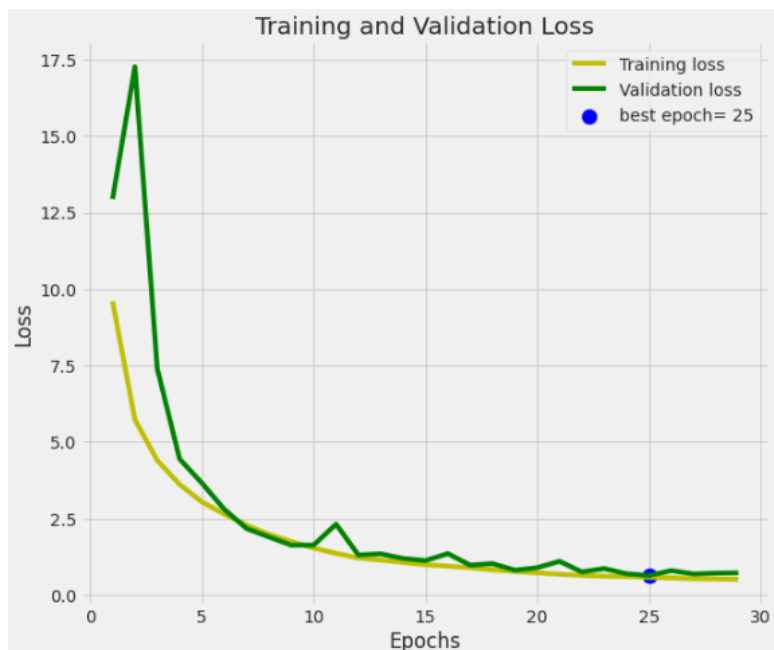


Fig 4.8: Training and validation loss graph for Densenet201 model.

As observed in Fig. 14, the loss graph for the Densenet201 model is displayed with regard to the number of epochs in the interval between 0 and 1 for 30 epochs. As time passes, we can observe decreasing training and validation loss. The training and validation loss was substantial in the early stages. However, as the number of epochs increases, the loss of training and validation decreases. The graph demonstrates that in the 25th epoch, the model experienced the least amount of loss.

The confusion matrix for EfficientNetB0 model is presented in Figure 15.

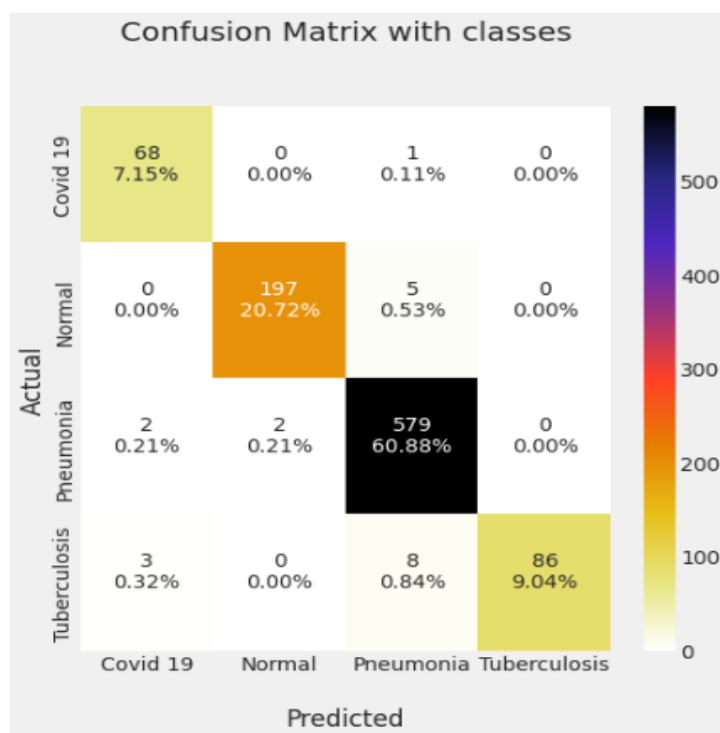


Fig. 4.9: Confusion matrix for Densenet201 Model

The confusion matrix produced by the suggested strategy is shown in 5*5 matrix. The result demonstrates that a set of 68, 197, 579 and 86 photos are correctly categorized by the proposed model as Covid-19, Normal, Pneumonia, and Tuberculosis type images. For the purpose of determining the results of the classifier, the values in Table 4.5.3.1 are modified in terms of TP, TN, FP, and FN. For the DenseNet169 model, the disease's inaccurate identification rate is noticeably reduced.

Table 4.6: Different classes TP, TN, FP, FN

Different Classes	Covid-19	Normal	Pneumonia	Tuberculosis
TP	68	197	579	86
TN	872	733	351	844
FP	5	2	14	0
FN	1	5	4	11

Table 4.7: Class-wise performance metrics for DenseNet201 model.

Model	Class	Precision	Recall	F1 Score	Accuracy
DenseNet201	Covid-19	0.93	0.99	0.96	0.98
	Normal	0.99	0.98	0.98	
	Pneumonia	0.98	0.99	0.99	
	Tuberculosis	1.00	0.89	0.94	

According to the table, we are able to deduce that the DenseNet201 model is capable of correctly identifying diseases with a rate of 98%, and the maximum precision reserved for the Pneumonia class.

CHAPTER 5

IMPACT ON SOCIETY, ENVIRONMENT AND SUSTAINABILITY

5.1 Impact on Society

Lung disease is a big reason why society as a whole has to pay so much money. This is true because it can lead to both disability and death at a young age. It also affects the direct costs of medical services and prescription drugs, as well as the indirect costs of lost productivity. In addition to these direct and indirect costs, respiratory disease is also linked to the huge costs of disability and loss of life-years. For both treating and preventing disease, it is important to find out what the risk factors are and limit exposure to them as much as possible. Public health and social actions are needed to reduce exposure to indoor smoke and other risk factors in order to come up with lung disease treatment plans that are both cost-effective and socially acceptable. This is needed to make protocols for how to treat pulmonary diseases. This is especially true in parts of the country where wages are low. This is of the utmost importance when dealing with situations where money is tight. This will lead to a more effective way to treat the person's illness. As a result of COVID-19-related cases of pneumonia, the number of adults with pneumonia has gone up. This could have long-term effects on many parts of a person's health, such as their neurological, cardiovascular, mental, and pulmonary health.

Most viral infections heal themselves or can be treated with antibiotics, and the patient doesn't need any other treatment besides supportive care to get better. These things made it hard to stop these deaths from happening. Lower respiratory tract infections are a leading cause of death and disability. If you want to lower your risk of dying or being unable to work, you must find these diseases early. To reach this goal, people in the community need to be informed and involved in the process. Exams, methods, and strategies in question must be able to tell the difference between bacterial, viral, and mycobacterial infections. Even in the most remote areas, morbidity and mortality rates must be lowered. This can only be done with techniques that are accurate, quick, and require only the most basic knowledge of technology. This study looks at how Deep Learning can be used to sort lung diseases into groups. As a direct result of our research, we were able to show how well it can detect the disease. This makes it less likely that someone will get the wrong diagnosis.

5.2 Impact on environment

By making use of deep learning, we will be able to classify a variety of respiratory disorders that fall under the purview of this inquiry. Some of these conditions include COVID-19, pneumonia, and tuberculosis. As an immediate and direct result of this, the illness will be much easier to recognize. There is a correlation between environmental exposures and the morbidity and mortality rates associated with lung illness. There are still information gaps in spite of the fact that legislation and education are being used to try to decrease the adverse effects of environmental exposures. Environmental factors, such as air pollution, have been linked to an increase in the risk of death from respiratory diseases and a worsening of respiratory symptoms, such as coughing, wheezing, and shortness of breath (shortness of breath).

Minority and socioeconomically disadvantaged communities are disproportionately affected by the respiratory disease loads that are present. This is because these communities are more likely to be exposed to air quality that is of a lower standard and to experience higher rates of respiratory prevalence and morbidity. Education has the potential to improve self-management among patients suffering from chronic respiratory illness, regardless of their socioeconomic position. This improvement may be achieved through the elimination of barriers to health literacy. Because of this improvement in self-management, there is a possibility that symptoms, as well as healthcare consumption and absenteeism, will decrease. This study will help to better understand the perceptions of environmental impacts on lung disease so that the effects of environmental exposures on symptoms can be better understood.

5.3 Sustainability Plan

The purpose of this research is to assist medical professionals in the diagnosis of lung disorders at an earlier stage. This model can be utilized by medicals and other professionals working in the health care industry to assist them in working more swiftly. Patients will benefit from this approach since it will reduce the likelihood of a wrong diagnosis being given to them, in addition to the fact that it is cost effective. Additionally, it will have an effect on the economy of our country.

CHAPTER 6

CONCLUSION AND FUTURE WORK

6.1 Conclusion

In this study, our primary objective was to identify Covid-19, Pneumonia, and Tuberculosis illness classifications from chest X-ray pictures, in addition to the Normal category. We employed a total of 6340 photographs for the experiment, dividing our data into three portions with an 80:15:5 ratio such that 5072 images could be used to train the model, 951 images could be used for the testing model, and 317 images could be used for validation. Because our dataset was insufficient, we decided to improve the photos by using an augmentation technique. During the course of our research, we utilized a number of distinct convolutional neural networks, including EfficientNetB0, DenseNet169, and DenseNet201. We decided to use chest X-ray images since it is a more cost-effective and time-efficient method, and accurate detection of the disease in its early stages is very crucial. The outcome achieved by our suggested model is quite remarkable. The levels of accuracy achieved by EfficientNetB0, DenseNet169, and DenseNet201 were respectively 99%, 99%, and 98%.

6.2 Scope and Limitations of the study

AI will usher in the fourth industrial revolution by enabling us to write programs more quickly. AI will thus be the era of the future. We won't be able to come up with any fresh ideas without AI. Everything will be automated with the aid of AI. We employed DNN and image processing in our study, and we believe that this will benefit those industries. Our research helps us develop knowledge and skills in the field of artificial intelligence while also advancing our grasp of deep learning techniques. The study provides ideas on how to address various image classification issues and extract characteristics from image files.

While conducting the research project, we faced a number of challenges. Images need more time and complexity to process than text or any other sort of data. High-end picture file handling tools are therefore necessary, but they are also rather expensive. It was challenging for us to collect these X-ray images. It was challenging for us to identify and collect validated data, so we used a variety of trustworthy sources. It was quite difficult for us to process the obtained data and feed the model without such inputs. To obtain excellent accuracy, we had to analyze the accuracy of several models, which required a lot of time.

6.3 Future Works

This research will be expanded in order to create a web application that will automate the disease identification process, thereby saving both time and money. Using this technology, physicians can examine the chest x-ray to determine if their conclusion was accurate. It can only aid physicians in making decisions; only an expert can make the final determination. Patients can also use the tool to determine if they have Covid-19, pneumonia, or Tuberculosis by downloading an X-ray image. They merely need to follow the doctor's instructions and, after the application identifies pneumonia, take the appropriate prescriptions. This strategy will aid in reducing the cost of pneumonia treatment, allowing disadvantaged individuals to receive adequate care at a reduced cost. It will alleviate some of the doctors' workload. This technique will allow doctors to treat more patients for less money, which would benefit everyone.

References

- [1] R. H. Abiyev and A. Ismail, "COVID-19 and Pneumonia Diagnosis in X-Ray Images Using Convolutional Neural Networks," *Math. Probl. Eng.*, vol. 2021, pp. 1–14, Nov. 2021, doi: 10.1155/2021/3281135.
- [2] L. Venkataramana, D. V. V. Prasad, S. Saraswathi, C. M. Mithumary, R. Karthikeyan, and N. Monika, "Classification of COVID-19 from tuberculosis and pneumonia using deep learning techniques," *Med. Biol. Eng. Comput.*, vol. 60, no. 9, pp. 2681–2691, Sep. 2022, doi: 10.1007/s11517-022-02632-x.
- [3] A. I. Khan, J. L. Shah, and M. M. Bhat, "CoroNet: A deep neural network for detection and diagnosis of COVID-19 from chest x-ray images," *Comput. Methods Programs Biomed.*, vol. 196, p. 105581, Nov. 2020, doi: 10.1016/j.cmpb.2020.105581.
- [4] A. N. Marginean *et al.*, "Reliable Learning with PDE-Based CNNs and DenseNets for Detecting COVID-19, Pneumonia, and Tuberculosis from Chest X-Ray Images," *Mathematics*, vol. 9, no. 4, p. 434, Feb. 2021, doi: 10.3390/math9040434.
- [5] World Health Organization, "Coronavirus." <https://www.who.int/health-topics/coronavirus> (accessed Nov. 10, 2022).
- [6] Google News, "Coronavirus (COVID-19)," *Google News*. <https://news.google.com/covid19/map?hl=en-US&gl=US&ceid=US:en> (accessed Nov. 10, 2022).
- [7] J. I.-Z. Chen, "Design of Accurate Classification of COVID-19 Disease in X-Ray Images Using Deep Learning Approach," *J. ISMAC*, vol. 2, no. 2, pp. 132–148, Jun. 2021, doi: 10.36548/jismac.2021.2.006.
- [8] L. Li *et al.*, "Using Artificial Intelligence to Detect COVID-19 and Community-acquired Pneumonia Based on Pulmonary CT: Evaluation of the Diagnostic Accuracy," *Radiology*, vol. 296, no. 2, pp. E65–E71, Aug. 2020, doi: 10.1148/radiol.2020200905.
- [9] M. Suzuki *et al.*, "A case of recurrent hemoptysis caused by pulmonary actinomycosis diagnosed using transbronchial lung biopsy after bronchial artery embolism and a brief review of the literature," *Ann. Transl. Med.*, vol. 7, no. 5, pp. 108–108, Mar. 2019, doi: 10.21037/atm.2019.02.11.
- [10] P. Reittner, S. Ward, L. Heyneman, T. Johkoh, and N. L. Müller, "Pneumonia: high-resolution CT findings in 114 patients," *Eur. Radiol.*, vol. 13, no. 3, pp. 515–521, Mar. 2003, doi: 10.1007/s00330-002-1490-3.
- [11] Star Health Desk, "Pneumonia in kids: Prevalence, prevention," *The Daily Star*, Feb. 15, 2022. <https://www.thedailystar.net/health/healthcare/news/pneumonia-kids-prevalence-prevention-2962116> (accessed Nov. 07, 2022).
- [12] World Health Organization, "Pneumonia." <https://www.who.int/news-room/fact-sheets/detail/pneumonia> (accessed Nov. 10, 2022).
- [13] Mayo Clinic, "Tuberculosis - Symptoms and causes - Mayo Clinic." <https://www.mayoclinic.org/diseases-conditions/tuberculosis/symptoms-causes/syc-20351250> (accessed Nov. 10, 2022).

- [14] “More than 100 people die of tuberculosis daily in Bangladesh,” *The Business Standard*, Aug. 24, 2022. <https://www.tbsnews.net/bangladesh/health/more-100-people-die-tuberculosis-daily-bangladesh-483202> (accessed Nov. 08, 2022).
- [15] D. Verma, C. Bose, N. Tufchi, K. Pant, V. Tripathi, and A. Thapliyal, “An efficient framework for identification of Tuberculosis and Pneumonia in chest X-ray images using Neural Network,” *Procedia Comput. Sci.*, vol. 171, pp. 217–224, 2020, doi: 10.1016/j.procs.2020.04.023.
- [16] T. Mehta and N. Mehendale, “Classification of X-ray images into COVID-19, pneumonia, and TB using cGAN and fine-tuned deep transfer learning models,” *Res. Biomed. Eng.*, vol. 37, no. 4, pp. 803–813, Dec. 2021, doi: 10.1007/s42600-021-00174-z.
- [17] S. H. Yoo *et al.*, “Deep Learning-Based Decision-Tree Classifier for COVID-19 Diagnosis From Chest X-ray Imaging,” *Front. Med.*, vol. 7, p. 427, Jul. 2020, doi: 10.3389/fmed.2020.00427.
- [18] U. Subramaniam, M. M. Subashini, D. Almakhles, A. Karthick, and S. Manoharan, “An Expert System for COVID-19 Infection Tracking in Lungs Using Image Processing and Deep Learning Techniques,” *BioMed Res. Int.*, vol. 2021, pp. 1–17, Nov. 2021, doi: 10.1155/2021/1896762.
- [19] J. I.-Z. Chen, “Design of Accurate Classification of COVID-19 Disease in X-Ray Images Using Deep Learning Approach,” *J. ISMAC*, vol. 2, no. 2, pp. 132–148, Jun. 2021, doi: 10.36548/jismac.2021.2.006.
- [20] T. B. Alakus and I. Turkoglu, “Comparison of deep learning approaches to predict COVID-19 infection,” *Chaos Solitons Fractals*, vol. 140, p. 110120, Nov. 2020, doi: 10.1016/j.chaos.2020.110120.
- [21] M. J. Horry *et al.*, “COVID-19 Detection Through Transfer Learning Using Multimodal Imaging Data,” *IEEE Access*, vol. 8, pp. 149808–149824, 2020, doi: 10.1109/ACCESS.2020.3016780.
- [22] Md. K. Mahbub, M. Biswas, L. Gaur, F. Alenezi, and K. Santosh, “Deep features to detect pulmonary abnormalities in chest X-rays due to infectious diseaseX: Covid-19, pneumonia, and tuberculosis,” *Inf. Sci.*, vol. 592, pp. 389–401, May 2022, doi: 10.1016/j.ins.2022.01.062.
- [23] M. Mamalakis *et al.*, “DenResCov-19: A deep transfer learning network for robust automatic classification of COVID-19, pneumonia, and tuberculosis from X-rays,” *Comput. Med. Imaging Graph.*, vol. 94, p. 102008, Dec. 2021, doi: 10.1016/j.compmedimag.2021.102008.
- [24] M. Zak and A. Krzyżak, “Classification of Lung Diseases Using Deep Learning Models,” in *Computational Science – ICCS 2020*, vol. 12139, V. V. Krzhizhanovskaya, G. Závodszy, M. H. Lees, J. J. Dongarra, P. M. A. Sloot, S. Brissos, and J. Teixeira, Eds. Cham: Springer International Publishing, 2020, pp. 621–634. doi: 10.1007/978-3-030-50420-5_47.
- [25] S. Bharati, P. Podder, and M. R. H. Mondal, “Hybrid deep learning for detecting lung diseases from X-ray images,” *Inform. Med. Unlocked*, vol. 20, p. 100391, 2020, doi: 10.1016/j.imu.2020.100391.

- [26] J. Anitha, M. Kalaiarasu, N. S. Kumar, and G. R. Sundar, "Detection and classification of lung diseases using deep learning," *AIP Conf. Proc.*, vol. 2519, no. 1, p. 030001, Oct. 2022, doi: 10.1063/5.0109980.
- [27] A. Soud, N. Sakli, and H. Sakli, "Classification and Predictions of Lung Diseases from Chest X-rays Using MobileNet V2," *Appl. Sci.*, vol. 11, no. 6, p. 2751, Mar. 2021, doi: 10.3390/app11062751.
- [28] S. Magrelli, P. Valentini, C. De Rose, R. Morello, and D. Buonsenso, "Classification of Lung Disease in Children by Using Lung Ultrasound Images and Deep Convolutional Neural Network," *Front. Physiol.*, vol. 12, p. 693448, Aug. 2021, doi: 10.3389/fphys.2021.693448.
- [29] D. Kermany, K. Zhang, and M. Goldbaum, "Labeled Optical Coherence Tomography (OCT) and Chest X-Ray Images for Classification," vol. 2, Jan. 2018, doi: 10.17632/rscbjbr9sj.2.
- [30] J. P. C. PhD, "ieee8023/covid-chestxray-dataset." Nov. 12, 2022. Accessed: Nov. 14, 2022. [Online]. Available: <https://github.com/ieee8023/covid-chestxray-dataset>
- [31] S. M. Islam and H. S. Mondal, "Image Enhancement Based Medical Image Analysis," in *2019 10th International Conference on Computing, Communication and Networking Technologies (ICCCNT)*, Kanpur, India, Jul. 2019, pp. 1–5. doi: 10.1109/ICCCNT45670.2019.8944910.
- [32] H. Mary Shyni and E. Chitra, "A comparative study of X-ray and CT images in COVID-19 detection using image processing and deep learning techniques," *Comput. Methods Programs Biomed. Update*, vol. 2, p. 100054, 2022, doi: 10.1016/j.cmpbup.2022.100054.
- [33] A. S. Gillis, "What is data splitting and why is it important?," *SearchEnterpriseAI*. <https://www.techtarget.com/searchenterpriseai/definition/data-splitting> (accessed Nov. 09, 2022).
- [34] S. Chatterjee, "What is Feature Extraction? Feature Extraction in Image Processing," *Great Learning Blog: Free Resources what Matters to shape your Career!*, Oct. 29, 2021. <https://www.mygreatlearning.com/blog/feature-extraction-in-image-processing/> (accessed Nov. 09, 2022).
- [35] "Feature Extraction." <https://www.mathworks.com/discovery/feature-extraction.html> (accessed Nov. 09, 2022).
- [36] T. Shermin, S. W. Teng, M. Murshed, G. Lu, F. Soheli, and M. Paul, "Enhanced Transfer Learning with ImageNet Trained Classification Layer." arXiv, Sep. 19, 2019. Accessed: Nov. 11, 2022. [Online]. Available: <http://arxiv.org/abs/1903.10150>
- [37] J. Deng, W. Dong, R. Socher, L.-J. Li, Kai Li, and Li Fei-Fei, "ImageNet: A large-scale hierarchical image database," in *2009 IEEE Conference on Computer Vision and Pattern Recognition*, Miami, FL, Jun. 2009, pp. 248–255. doi: 10.1109/CVPR.2009.5206848.
- [38] A. Borad, "Image Classification with EfficientNet: Better performance with computational efficiency," *Medium*, Jul. 10, 2021. <https://datamonje.medium.com/image-classification-with-efficientnet-better-performance-with-computational-efficiency-f480fdb00ac6> (accessed Nov. 11, 2022).

- [39] M. Tan and Q. V. Le, “EfficientNet: Rethinking Model Scaling for Convolutional Neural Networks.” arXiv, Sep. 11, 2020. Accessed: Nov. 11, 2022. [Online]. Available: <http://arxiv.org/abs/1905.11946>
- [40] G. Huang, Z. Liu, L. van der Maaten, and K. Q. Weinberger, “Densely Connected Convolutional Networks.” arXiv, Jan. 28, 2018. Accessed: Nov. 13, 2022. [Online]. Available: <http://arxiv.org/abs/1608.06993>
- [41] A. Narin, C. Kaya, and Z. Pamuk, “Automatic detection of coronavirus disease (COVID-19) using X-ray images and deep convolutional neural networks,” *Pattern Anal. Appl.*, vol. 24, no. 3, pp. 1207–1220, Aug. 2021, doi: 10.1007/s10044-021-00984-y.
- [42] H. Mukherjee, S. Ghosh, A. Dhar, S. M. Obaidullah, K. C. Santosh, and K. Roy, “Deep neural network to detect COVID-19: one architecture for both CT Scans and Chest X-rays,” *Appl. Intell.*, vol. 51, no. 5, pp. 2777–2789, May 2021, doi: 10.1007/s10489-020-01943-6.
- [43] P. Baheti, “Activation Functions in Neural Networks [12 Types & Use Cases].” <https://www.v7labs.com/blog/neural-networks-activation-functions>, <https://www.v7labs.com/blog/neural-networks-activation-functions> (accessed Nov. 11, 2022).

Runa Akter 221-25-110_lung diseases

ORIGINALITY REPORT

12% SIMILARITY INDEX	8% INTERNET SOURCES	8% PUBLICATIONS	2% STUDENT PAPERS
--------------------------------	-------------------------------	---------------------------	-----------------------------

PRIMARY SOURCES

1	www.ncbi.nlm.nih.gov Internet Source	2%
2	dspace.daffodilvarsity.edu.bd:8080 Internet Source	1%
3	www.mdpi.com Internet Source	1%
4	Mahmoud Bakr, Sayed Abdel-Gaber, Mona Nasr, Maryam Hazman. " <u>DenseNet Based Model for Plant Diseases Diagnosis</u> ", European Journal of Electrical Engineering and Computer Science, 2022 Publication	1%
5	www.researchgate.net Internet Source	1%
6	koreascience.kr Internet Source	1%
7	<u>Rahib H. Abiyev</u> , Abdullahi Ismail. "COVID-19 and Pneumonia Diagnosis in X-Ray Images Using Convolutional Neural Networks", Mathematical Problems in Engineering, 2021	<1%